FLOWING FROM RELEASE TO RUNOUT: HIGH-RESOLUTION RADAR MEASUREMENTS OF SNOW AVALANCHES

Anselm Köhler[1,*], Michael Neuhauser[1], Gregoire Bobillier[2], Jan-Thomas Fischer[1]

[1] *Department for Natural Hazards, Austrian Research Centre for Forests, Innsbruck, Austria*
[2] *WSL Institute for Snow and Avalanche Research SLF, Davos, Switzerland*

ABSTRACT: Radar technology is indispensable in the context of snow avalanche monitoring. Practitioners rely on the capabilities of related real-time detection systems while scientists use radar for high resolution measurements. In combination with other measurement systems, radar provides an important reference: For example, neither in-flow nor single point measurements can be solely used to interpret the avalanche flow evolution in a holistic view without the reference that radar systems provide. Radar data yield a multitude of details from release to avalanche flow and final deposition. Today, this information is rarely used in practice as the processing requires manual steps but is invaluable from a scientific point of view. We present radar data of the newly developed frequency modulated radar mGEODAR, which is deployed at the Nordkette test-site above Innsbruck, Austria, and recorded data on nearly 200 avalanches since 2021. The avalanches range from very small to large size and corresponding flow regimes are mostly dry-dense with the largest ones reaching the transition towards powder snow avalanche flow. During the release, the radar's high spatial and temporal resolution allows us to infere weak layer crack propagation speeds in the context of snow slab avalanche initiation after an artificial trigger. We obtained crack propagation speeds in the up-slope and down-slope directions up to 100m/s, which is in line with the recent literature values measured from camera-based full-scale slab avalanches and numerical modeling of propagation saw tests. During the flow phase, we track the evolution of the avalanche front velocity that typically reaches up to 30m/s, and show the application of the front data for avalanche flow model evaluation. Especially during the deposition, the radar signatures allow to distinguish the stopping behavior and to differentiate between cold and warm flow regimes. The presented radar datasets provide a valuable source for future research covering the improvement of automatic and machine learning supported classification, filtering and spectral processing, as well as snow and avalanche science related research questions regarding the avalanche flow evolution and dependence on weather and snowpack patterns.

Keywords: Avalanche dynamics, radar measurements, weak layer crack propagation speed, front velocity.

1. INTRODUCTION

Radar measurements became the defacto standard as overview reference in the currently active full-scale avalanche dynamics test-sites Vallée de la Sionne (Vdls) (Köhler et al., 2018b) and Ryggfonn (Gauer and Kristensen, 2016). Radar measurements enable to bring local point measurements into the context of the full avalanche from head to tail, since the whole flow evolution from release to deposition is captured. Which information is contained in the radar data, i. e. velocity spectrum or position, depends on the radar type. Generally, radar devices classify based on their signal characteristic: pure Doppler radars resolve only velocities within the field of view (Salm and Gubler, 1985); pulse-Doppler radars track velocities in range-gate with tens of metres resolution (Schreiber et al., 2001);and frequency-modulated systems known as FMCW radars primarily resolve position with sub-metre resolution at more than 100 Hz pulse rate (Ash et al., 2010).

In contrast to radar systems in operational use for detection, the requirement on radars for research purposes are generally higher spatial and temporal resolution in tradeoff with processing time. All commercially available radars are limited in their spatial resolution due to national frequency regulations for continuous operation, thus purpose-made radars with sub-metre resolution are prefered for reseach. The herein presented FMCW-type radar system *mGEODAR* is in development since 2018 (Köhler et al., 2020) and matured to a reliable system in its current Mark II. Together with the mGEODAR development, the avalanche test-site *Nordkette* above Innsbruck, Austria, has been reestablished, and 185 avalanches have been recorded since winter season 2020/21 (Fig. 1).

Distinct signatures in the radar data have been iden-

*Corresponding author address:
Anselm Köhler, Department for Natural Hazards,
Austrian Research Centre for Forests (BFW);
6020 Innsbruck, Austria;
tel: +43 664 8850 8304;
email: anselm.koehler@bfw.gv.at

tified and used for a flow regime classification of snow (Köhler et al., 2018b). The radar signatures show that avalanches establish 7 flow regimes and 3 stopping mechanisms, enhancing on the conventional dichotomy between dense flow avalanche and powder snow avalanche (Faug et al., 2018). A shortcoming of the flow regime definition relies in the fact that only the unique prototype radar GEODAR pointing towards the single avalanche track of VdlS was used. Here we show, that the mGEODAR radar data from the Nordkette topography include the same distinct signatures and supports the existance of the flow regimes.

Beside radar signatures of flow regimes, the data contain the outline of an avalanche as line features which includes the leading and tailing edge as well as surges inside the avalanche. In the vicinity of the triggering explosion, the leading edge in the radar appear rapidly over a larger area. We hypothesis the changes in the radar signal corresponds to movements of the snow surface which is assumed to relate to the crack propagation inside a weaklayer. Crack propagation speed are reported to range between 10 and up to 250 m/s (Simenhois et al., 2023). Image correlation techniques allow to track markers or speckle patterns on the side of snow columns in propagation saw tests (PST) configuration, e.g. isolated snowpack blocks of less than 5 m length, and find velocities up to 20–30 m/s that are in the range with the anti-crack model that describes a collapse of the slab (Heierli et al., 2011). Early work by manual video frame analysis of tracking the crack opening on full scale avalanche releases find considerable larger velocities of 50–100 m/s (Hamre et al., 2014). By collating data from image correlation method on larger PST, accelerometer measurements on top of the snowpack and manual video analysis of an exceptional case of crack propagation, Bergfeld et al. (2022) find a scale dependence towards higher crack propagation velocities for larger fracture lengths. Such large difference in measured crack propagation speeds are reproduced using numerical models, and recently classified into slow collapse-driven and supersonic shear-driven crack propagation modes (Bobillier et al., 2024). Still, measurements on real avalanche scale are rare due to reliance on good visibility and high-quality video footage of the release. We show evidence and discuss that the mGEODAR radar is able to measure the crack propagation speed.

The radar data, and in particular the velocity of the front, are used for evaluation and parameter optimization Avalanche simulation tools. Currently, the features like the front are extracted manually from the data as position over time. This gives a certain subjectivity, but also the conversion to a front velocity by time derivation amplifies errors. In terms of dynamic avalanche model evalution, we show how to prevent this by directly fitting the simulation result to the front position data in the coordinate system of the radar. Such process can also be seen as a model-based data smoothing approach and together with maschine-learning based data analysis will become useful in the future. The growing data repository with labeled avalanche data facilitates on that.

The structure of the paper starts by introducing the test-site Nordkette and the radar mGEODAR, together with the relevant processing steps (Sec. 2.). The results contain a description of the avalanche data and flow regime signatures (Sec. 3.1 & 3.2). A discussion on the radar information on crack propagation speed is followed by an example how the radar data can be used for numerical avalanche model validation (Sec. 3.3 & 3.4).

2. METHODS

2.1 Test-site & Radar

The avalanche measurements with the mGEODAR radar are performed at the Nordkette ski resort above Innsbruck, Austria (Lat: 47.306591, Lon: 11.379889, WGS84, Fig. 1). Avalanche control work with remote avalanche control systems (rope ways and gas exploders) is performed after each snow fall or strong snow drift into the release areas to ensure safety for the ski slopes and infrastructure. Numerous release locations are spread over the whole catchment and the main release areas are named *Kaminspitze*, *Mittelrinne*, *Karrinne*, *Juliusrinne* and *Seilbahnrinne*. Smaller areas are known as *Wasserschloss* and at the gas exploder locations (Fig. 1A). The main advantages of this test-site are the frequent avalanche releases due to an average sum of yearly snow fall up to 20 m and the save access from the city center, rendering it ideal for sensor prototype development and testing.

The radar mGEODAR has a limited antenna aperture of 10° horizontal, but covers the whole mountain from top to bottom with 90° vertical aperture. This means, that only parts of the catchment can be monitored at one time. Throughout the years, the radar was installed at two locations B and A with different orientations 1-3: Season 2020/21 orientation B2, Season 2021/22 orientation A3, Season 2022/2023 orientation B1 and Season 2023/24 orientation A3 (Fig. 1A).

The mGEODAR radar hardware is loosely related to the GEODAR Mark IV radar (Tanha et al., 2017),

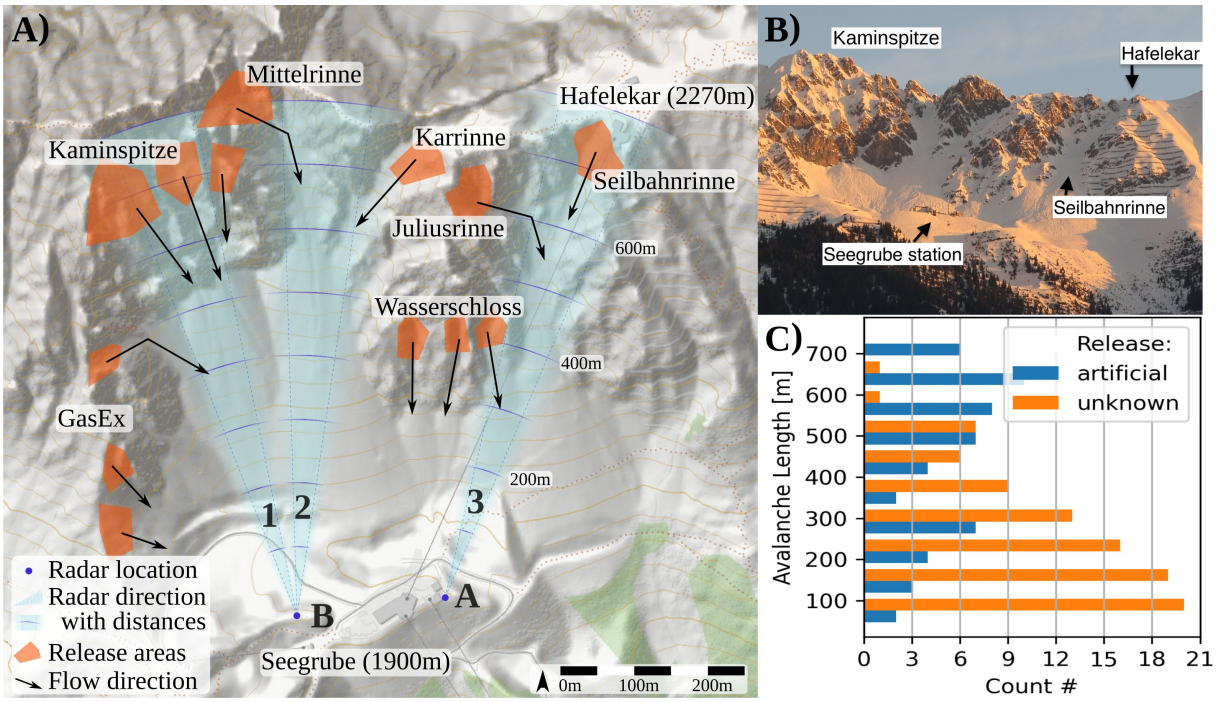

Figure 1: Overview of avalanche test-site Nordkette. A) Topographic map with radar locations B1, B2 and A3, and the different blasting locations and release areas. B) Picture taken from southern direction. C) Histogram of release to deposition distance (avalanche length) from avalanche data of winter seasons 2020/21 to 2023/24.

and the system has 0.35 cm range resolution with currently 100 Hz pulse rate and a theoretical maximum range of 3.5 km. A main difference to the predecessor GEODAR is the use of 10 Ghz instead of 5 GHz, and correspondingly the wavelength of 2.5 cm is more sensitive to smaller particles. The powder cloud and snowfall should be still transparent to the mGEODAR, however, it seems to miss sharpness in the avalanche signatures compared to the predecessor radar (Fig. 3.2). More technical details are found in Köhler et al. (2020).

The radar is not running continously over the season, but is manually controlled each morning when the snow situtation requires avalanche control. Therefore natural avalanche activity is not the main focus of the test-site, but the radar can be turned on when specific weather situations like strong snowfall, rain-on-snow or intense solar radiation render natural avalanches likely.

2.2 Radar data processing

The initial processing step is Fourier analysis of the data from a single FMCW pulses, which converts them into amplitude values as a function of range (line-of-sight distance). A series of pulses then track changes in the scene over time. The amplitude-over-range signal includes contributions from any object within the field of view that is larger than the 2.5 cm wavelength. These contributions consist of static signals from features such as the mountain and snow cover, as well as signals from moving objects like gondolas, skiers or avalanches.

A crucial step in the processing workflow is the separation of static and moving objects, along with the normalization to compensate for attenuation with range. To achieve this, a moving target identification (MTI) filter is applied, which enhances pulse-to-pulse changes over 0.1 s (a sequence of 10 pulses) by calculating the rolling standard deviation of the amplitude signal at each range. The resulting signal is then normalized to periods when no motion is detected in the scene, typically a few seconds before an avalanche event. Compared to previously used MTI filters based on high-pass filtering (Köhler et al., 2018b), the rolling standard deviation filter offers improved clarity, particularly for the onset and leading edge of an avalanche.

2.3 Feature and signature extraction

The processed data are presented in range-time diagrams, where the color scale represents the MTI intensity in decibels. The slope of features in these diagrams directly corresponds to the approach velocity, indicating how fast flow structures or objects are moving towards the radar. This is not neccessary the path-parallel velocity of an avalanche depending on the alignment of the radar to the

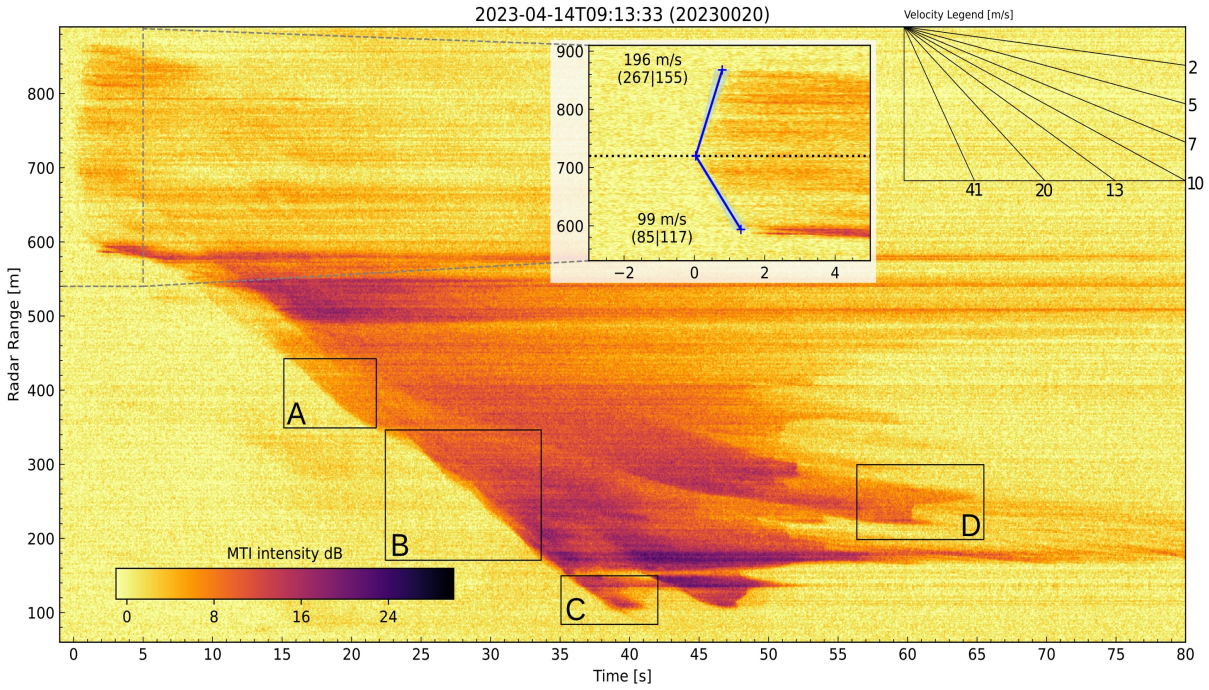

Figure 2: Avalanche #20230020 from Kaminspitz release area (B1, Fig. 1) with multiple surges. The radar signatures indicate the existence of several flow regimes within this one avalanche. A zoom on the release over 270 m range is given in the inset.

avalanche track. At Nordkette, the radar underestimates the avalanche velocity by around 10 %.

The extraction of features like the onset, leading edge and flowing surges from the data is done manually by hand picking for each avalanche. The advantage is a precise control in noisy sections, but with the trade-off of subjectivity. The manually extracted features are the basis for annotated datasets for future work on automated extraction algorithms. The identification of signatures of flow regimes is also a qualitative process based on the MTI plots.

3. RESULTS & DISCUSSION

3.1 Avalanche data

The avalanches observed at the Nordkette site are typically classified below destructive size class III, as the vertical drop is less than 400 m (Fig.1A). A brief summary of all recorded avalanches is presented in Figure 1C, which includes a histogram of avalanche lengths. Here, avalanche length refers to the range difference between the furthest and closest occurence of the avalanche signal in the radar data. It is important to note that this radar based length serves as a proxy for the actual 3D travel length, due to geometric factors such as the alignment offset between the radar line of sight and the avalanche track. Despite this limitation, confirmed artificially triggered avalanches exhibit flow lengths of up to 700 m, while naturally occurring avalanches are concentrated at lengths below 300 m.

Most recorded avalanches are released during storm periods with heavy precipitation and cold temperatures leading to cold-dense avalanches. Visibility constraints allowed for video recording on only a few days, making visual references for most of the dataset unavailable. The few available videos indicate that the avalanches are just about to transform towards powder snow avalanches with an intermittent frontal region (Sovilla et al., 2018). The Nordkette avalanche data will contribute to understanding the factors driving this critical transition.

All radar data will be made publicly available through the BFW community on the Zenodo data repository[1]. The numbering scheme contains the second year of the season and a running number, similar to the numbering system of the Swiss test-site Vallee de la Sionne. We encurage interested readers to check for ongoing uploads of yearly reports. These radar datasets, along with supplementary information, form the basis for evaluating avalanche dynamic models, as demonstrated in Section 3.4. The data repository also supports improvements in the processing algorithms and automatic feature extraction using the manually labeled data segments.

[1] https://zenodo.org/communities/bfw-data

3.2 Flow regime signatures

Figure 2 shows avalanche #20230020 from season 2022/2023 that released below the Kaminspitz above a steep rock face (Fig. 1B). The avalanche was triggered at 9:13 in mid of April after 70 cm of new snow at the Seegrube. By this time, the air temperature was little below zero and the diffuse solar radiation caused the snow on the southern slopes to moisten. The lowermost 20 cm of the new snow was isotherm with a density around 200 kg/m^3. The location of the blast is at 720 m range and the total release area spreads from 600 m to 870 m range. The release did not happen instantaneous, but takes around one second to reach the upper and lower extend. We interpret this as the release of a slab. The leading edge of the avalanche accelerates during the first 5 s, continues with a steady velocity of 20 m/s until the beginning of markup B in Figure 2, and continues with velocities up to 30 m/s in several frontal surges until the deposition at 100 m range.

The following interpretations compare the features and signatures against the flow regimes identified by Köhler et al. (2018b). Markup A highlights a frontal area that has a homogenouos radar signature, indicating a flow without much internal structure and has been previously identified as a cold-dense flow regime. Later at markup B, the leading edge becomes wavy and forms surges that overtake each other. Possibly, this marks the transition towards a powder snow avalanche with an intermittent flow regime. It is important to note, that the signature of the intermittent regime does not contain as many streaks as it is known from the predecessor radar GEODAR. The reason could be, that the mGEODAR uses higher frequency and picks up more signal from the powder cloud which might smear the signal of the unterlying flow structures.

Nevertheless, the following starving stopping mechanism in markup C fits well to the previous flow regimes, as it is know from mostly cold flows. Already the stopping signature of the second surge (just right of markup C) shows a more pronounced backward propagating stopping shock known from warm shear flows. The following tail, that leads to markup D, is with 5 m/s clearly slower than the front (see velocity legend in Fig. 2). Its stopping signature shows an abrupt stopping over 40 m which is well known to happen in warm plug flows (Köhler et al., 2018a).

The existence of several flow regimes in one avalanche are recognized before. A reason for that might be a separation of the snow types leading to colder snow at the front. Warmer snow is generally found lower in the snowpack, and its entrainment by sort of gradual erosion is achieved behind the front. Actually, the warm plug surge from markup D appears faintly already in markup A at 420 m. The surge never reaches the velocity of the front and constantly separates from it.

Not all avalanches from the Nordkette test-site show a similar complexity of the flow. Most avalanches are of a pure cold-dense type. This is attributed to the fact, that artificial releases are usually performed after significant amount of new snow during the peak winter season when cold temperatures preveal. However, when lots of new snow accumulate over the course of the night, the avalanches can grow in size and mark the transition towards powder snow avalanches. Investigation of this transitions and driving factors thereof is still an important knowledge gap.

3.3 Crack propagation speed

In season 2021-2022 and season 2023-2024, the radar points towards the couloir Seilbahnrinne (A3 in Fig. 1). The terrain is confined and the flow path is in line with the radar line of sight. The blast location is inside the radar viewshed at a range of around 720 m and eight avalanches indicate that their release happens quickly over up to 160 m range, e. g. potentially due to a slab release (Fig. 3). Unfortunately no video data from the release area exist due to bad visibility.

The radar data of the Mittelrinne release area (B2 in Fig. 1) was not taken into account because of limited view into the release area even though several datasets show similar rapid releases over a large area. However, a video of 2021-01-15 (#20210048) shows that the shock wave from the detonation releases sluff in the surrounding rock faces, which is also faintly visible in the radar data. Without good quality video, this release area is not suited for interpretion of the release mechanism due to the very complex terrain and interaction of the shock wave with it.

At Seilbahnrinne, the blasting location is close to the end of the couloir at a height of up to 10 m above the snow cover depending on the amount of snow. Above, the couloir steepens up so that a direct shock wave hits the upper couloir flanks in a steep angle. These upper zones are at a maximum distance of 760 m and well in the effective radius of a over-snow detonation. The speed of a shock wave due to an over-snow detonation approaches towards the speed of sound (340 m/s) for distances larger than 10–15 m (Simioni et al., 2015). For most of the datasets in Table 1, the upward direction from

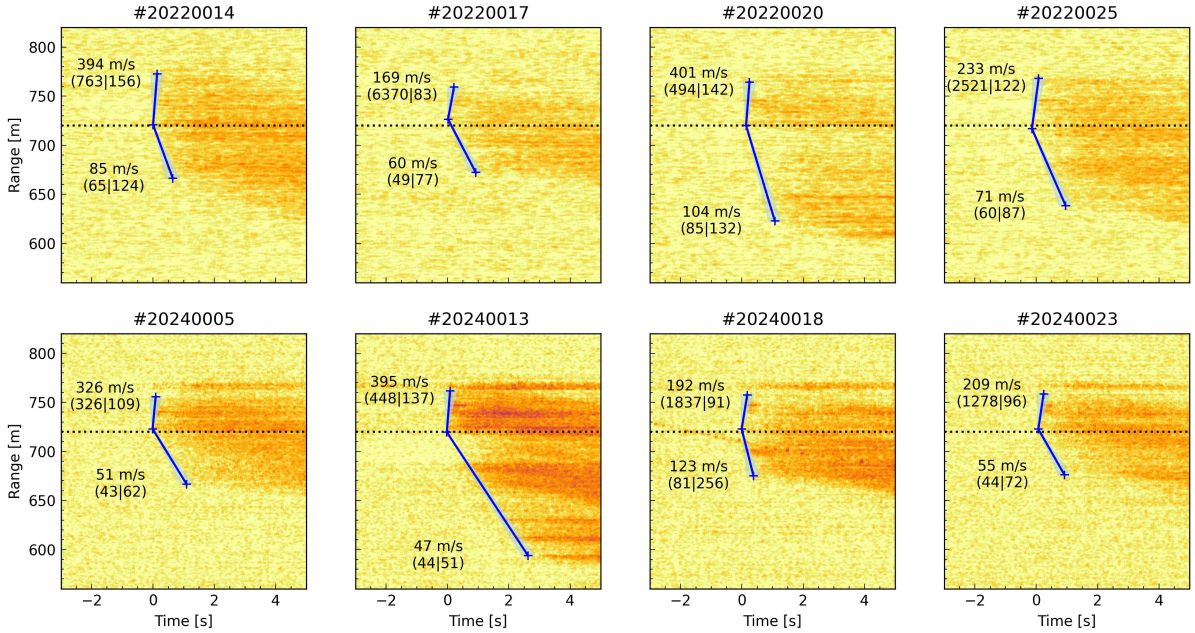

Figure 3: Zoom on the release of 8 avalanche dataset from season 2021/2022 and 2023/2024. Blue lines are the manually picked fronts with ±0.2 s second cone of error in light blue, of which the velocities are indicated with text and span of velocity error in brackets.

the blast locations give high velocities in this range. Note that the estimation of those high velocities are prone to large error as discussed later.

In the downward direction from the blast location, the release signatures in the radar data reach up to 120 m further. All estimated velocities are significantly lower than the speed of the shock wave. The velocities are in the order of 50 m/s to 100 m/s, which is well in the range of previously reported measurements (Bergfeld et al., 2022)

There are a few avalanche dataset from the Seilbahnrinne release area that do not show a similar release signature. Their release signature spreads over less than 100 m only and a direct release due to the detonation is likely. Similar is the release of avalanche #20240014 from the Wasserschloss release area (Fig. 1) at distance of 390 m. Due to the closer range, the signal of the release is stronger than for the other avalanche dataset, and clearly show release speed of similar order of the shock wave.

Table 1: Table of properties for identified crack propagation speed of ranges r [m] and velocities v [m/s] for upwards ($_u$) and downward ($_d$) direction from blast location r_b. Radar location for #2022 & #2024 = A3 and #2023 = B1.

Aval. Nr	r_u	r_d	r_b	v_u	v_d
20220014	773	666	721	394	85
20220017	759	672	726	169	60
20220020	764	623	720	401	104
20220025	768	638	717	233	71
20240005	756	667	723	326	51
20240013	762	594	720	395	47
20240018	758	675	723	192	123
20240023	759	676	723	209	55
20240014	411	358	386	193	269
20230020	868	594	720	196	99

It is important to mention, that most of the identified crack release signatures have only a faint signal. From a radar point of view, the small change of the weak layer collapse is much smaller than the range resolution of 35 cm or wave length of 2.5 cm. An interferometric radar that utilizes phase processing of the incoming electromagnetic wave would be better tool for tracking of small changes but its temporal resolution is too small. To which extend an phase-sensitive MTI filter improves upon the herein used rolling magnitude-only standard deviation filter, is yet to be tested.

Avalanche #20230020 in Figure 3.2 is an very impressive release below the Kaminspitze. From the blast location at 720 m, the weak layer fracture propagates towards the mountain crest at 870 m and the rock face at 600 m, and a slab with 270 m extend is released (a half of the trajectory length). A release due to the direct shock wave is not plausible due to the large size of the release and topography with small ravines and ridges (Fig. 1B). The propagation happens with speeds up to roughly 200 m/s.

The accuracy of the velocity estimate is dependent

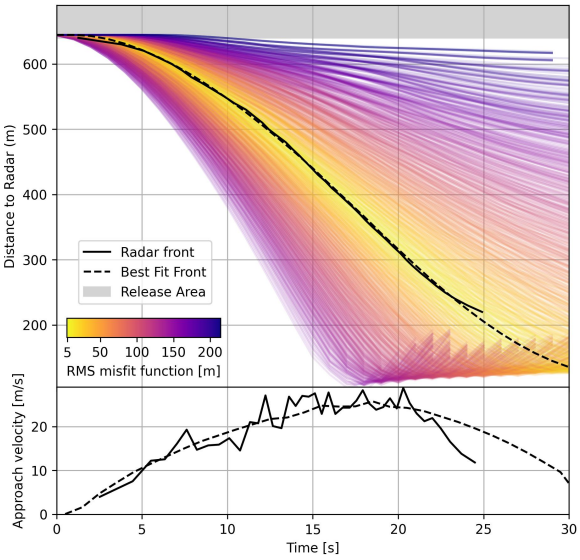

Figure 4: Example of model evaluation using the front data from the radar (black line). Colored lines are the misfit between data and the foremost point (fronts) from 1050 simulations in radar coordinates. The best fit (black dashed) simulation yields in a physics-informed model-based smoothing of the front data (lower panel).

upon the precision of manual hand-picking. Small errors in manual picking can lead to significant deviations, especially at higher velocities. For instance, considering a propagation distance of 100 m with a picking error of ±0.2 s, the resulting velocities range from 45 to 55 m/s for picking uncertainties between 1.8 and 2.2 s, from 83 to 125 m/s for times between 0.8 and 1.2 s, and from 143 to 333 m/s for times between 0.3 and 0.7 s (Fig. 3). Evidently, for velocities exceeding 150 m/s along such a short distance, any velocity estimation is not reliable.

3.4 Model evaluation with radar data

Even at velocities in the range of the front that are usually below 30 m/s for the Nordkette, the velocity uncertainty from taking the time derivative of tracked line features in the range-time diagrams is not neglectable (lower panel, Fig. 4). It is therefore advisable to directly fit the front position data over time to estimate parameters of numerical avalanche models, instead of optimizing for velocities (Rauter and Köhler, 2019; Neuhauser et al., in submission). A misfit function to find best-fit model parameters can consist of the root mean square difference between the measured and the simulated front position over time in radar range coordinates. Basically, the simulation exports the results as synthetic radar range-time data. The benefit is that this step automatically applies any geometric corrections to the radar data to compensate for misalignment of the radar beam with the true avalanche flow path. The upward directed simulated fronts in Figure 4 at ranges below 200 m impressively demonstrate these geometric effects and yield in increasing ranges with time after the avalanche passes to the side of the radar (compare with flow path in Seilbahnrinne that turns south after the steep couloirs, Fig. 1A/B).

The open-source digital toolbox for avalanche simulations *AvaFrame* (Oesterle et al., 2022) conviently includes all neccessary transformation and export tools. 1050 simulations have been calculated to cover a descent region of the model's parameter space. The best-fit simulation reaches a misfit of only 4.4 m for all timesteps between 0–25 s, i. e. 1 % of the total range covered by the avalanche. Afterwards the avalanche moves out of sight of the radar antenna aperture.

Such a fitting process can be also seen as a physics-informed model-based smoothing of the manually picked front positions (lower panel Fig. 4). However, employing such an advanced model, e. g. the thickness integrated flow model com1DFA calculates a flow on 3D topography, solely for smoothing of the data comes with high computational costs. But simpler models that run on 2D path-following topographies loose the capapilities of the geometric transformations.

3.5 Automatic feature extraction

Interpreting radar data is challenging and ideally should be coupled with visual confirmation from video. Limitations arise from the lack of lateral resolution and the subjective nature of manual feature extraction. One approach to address these challenges is by generating digital twins of the radar data using numerical avalanche models. In the future, the radar data repository together with the manual labels of the avalanche front and outline supports the development of automatic, physics-informed and maschine learning-based algorithms for feature and signature extraction and interpretation.

From an operational perspective, such advanced methods for avalanche detection in radar data may not always be necessary. However, these advancements could offer benefits for situation dependent detection and alarming routines. For example, imagine a avalanche track leading to a busy road that crosses the deposition area. Most of the detected avalanches tend to stop before reaching the road, so the alarming routines should be tuned to minimize unnecessary road closures. Currently, most approaches close the road as soon as the avalanche reaches a certain range to allow for enough time to the cars for road clearing. When the avalanche did not reach the road, the system

can automatically reopen the road. Real-time information on the velocity evolution, the dominant flow regime, the avalanche mass and an increase thereof, could enable a more precise prediction if the road is endangered and facilitate appropriate responses of the alarming routines.

4. CONCLUSION

This study on high-resolution radar measurements with mGEODAR of snow avalanches at the Nordkette test-site yields three key findings. Beside front velocities, flow regime signatures and internal flow features, the radar reveals information on weak layer crack propagation speeds by temporal tracking of signal changes during snow slab avalanche initiation. The measured speeds reach up to 100 m/s, which align with recent literature. Compared to measurements based on video, the radar measurements do not rely on good visibilies during the release. The radar system effectively tracks the avalanche front with sub-metre resolution at 100 Hz. These dynamic data are critical for validating and refining avalanche flow models, enhancing our understanding of avalanche dynamics and improving the predictive accuracy. Typical radar signatures allow for detailed classification of avalanche flow regimes and stopping behaviors. Especially the Nordkette test-site has a suitable size to investigate the transition from a cold-dense to the intermittent flow regime known from powder snow avalanches. The data repository will support future research and development, and offers a valuable resource for automatic and machine learning-based radar analysis. The data are constantly made available through the BFW community on Zenodo.

ACKNOWLEDGEMENT

We thank the Nordkette Ski resort and avalanche commission for their invaluable support and collaboration in data collection for this study.

References

Ash, M., Brennan, P. V., Chetty, K., McElwaine, J. N., and Keylock, C. J.: FMCW Radar Imaging of Avalanche-like Snow Movements, in: Proceedings of the 2010 IEEE Radar Conf., pp. 102–107, IEEE, Arlington, Va., doi:10.1109/RADAR.2010.5494643, 2010.

Bergfeld, B., van Herwijnen, A., Bobillier, G., Larose, E., Moreau, L., Trottet, B., Gaume, J., Cathomen, J., Dual, J., and Schweizer, J.: Crack propagation speeds in weak snowpack layers, Journal of Glaciology, 68, 557–570, doi:10.1017/jog.2021.118, 2022.

Bobillier, G., Trottet, B., Bergfeld, B., Simenhois, R., van Herwijnen, A., Schweizer, J., and Gaume, J.: Supershear crack propagation in snow slab avalanche release: new insights from numerical simulations and field measurements, Natural Hazards and Earth System Sciences Discussions, 2024, 1–15, doi:10.5194/nhess-2024-70, 2024.

Faug, T., Turnbull, B., and Gauer, P.: Looking beyond the powder/dense flow avalanche dichotomy, Journal of Geophysical Research: Earth Surface, 123, 1183–1186, doi:10.1002/2018jf004665, 2018.

Gauer, P. and Kristensen, K.: Four decades of observations from NGI's full-scale avalanche test site Ryggfonn—Summary of experimental results, Cold Regions Science and Technology, 125, 162–176, doi:10.1016/j.coldregions.2016.02.009, 2016.

Hamre, D., Simenhois, R., and Birkeland, K. W.: Fracture Speeds of Triggered Avalanches, URL https://arc.lib.montana.edu/snow-science/item/2048, 2014.

Heierli, J., Birkeland, K., Simenhois, R., and Gumbsch, P.: Anticrack model for skier triggering of slab avalanches, Cold Regions Science and Technology, 65, 372–381, doi:10.1016/j.coldregions.2010.10.008, 2011.

Köhler, A., Fischer, J.-T., Scandroglio, R., Bavay, M., McElwaine, J., and Sovilla, B.: Cold-to-warm flow regime transition in snow avalanches, The Cryosphere, 12, 3759–3774, doi:10.5194/tc-12-3759-2018, 2018a.

Köhler, A., McElwaine, J., and Sovilla, B.: GEODAR data and the flow regimes of snow avalanches., Journal of geophysical research: earth surface., 123, 1272–1294, doi:10.1002/2017jf004375, 2018b.

Köhler, A., Lok, L. B., Felbermayr, S., Peters, N., Brennan, P. V., and Fischer, J.-T.: mGEODAR—A Mobile Radar System for Detection and Monitoring of Gravitational Mass-Movements, Sensors, 20, 6373, doi:10.3390/s20216373, 2020.

Neuhauser, M., Köhler, A., Wirbel, A., Dressler, F., Fellin, W., and Fischer, J.-T.: Particle and front tracking in experimental and computational avalanche dynamics, Natural Hazards and Earth System Science, in submission.

Oesterle, F., Wirbel, A., Tonnel, M., and Fischer, J.-T.: avaframe/AvaFrame: latest Version, doi:10.5281/zenodo.4721446, 2022.

Rauter, M. and Köhler, A.: Constraints on Entrainment and Deposition Models in Avalanche Simulations from High-Resolution Radar Data, Geosciences, 10, doi:10.3390/geosciences10010009, 2019.

Salm, B. and Gubler, H.: Measurement and analysis of the motion of dense flow avalanches, Annals of Glaciology, 6, 26–34, doi:10.1017/s0260305500009939, 1985.

Schreiber, H., Randeu, W. L., Schaffhauser, H., and Rammer, L.: Avalanche dynamics measurement by pulsed Doppler radar, Annals of Glaciology, Vol 32, 2001, 32, 275–280, doi:10.3189/172756401781819021, 2001.

Simenhois, R., Birkeland, K. W., Gaume, J., van Herwijnen, A., Bergfeld, B., Trottet, B., and Greene, E.: Using video detection of snow surface movements to estimate weak layer crack propagation speeds, Annals of Glaciology, p. 1–11, doi:10.1017/aog.2023.36, 2023.

Simioni, S., Sidler, R., Dual, J., and Schweizer, J.: Field measurements of snowpack response to explosive loading, Cold Regions Science and Technology, 120, 179–190, doi:10.1016/j.coldregions.2015.06.011, 2015.

Sovilla, B., McElwaine, J., and Köhler, A.: The Intermittency Regions of Powder Snow Avalanches, Journal of Geophysical Research (Earth Surface), 123, 2525–2545, doi:10.1029/2018jf004678, 2018.

Tanha, M. A., Brennan, P. V., Ash, M., Köhler, A., and McElwaine, J. N.: Overlapped Phased Array Antenna for Avalanche Radar, 65, 4017–4026, doi:10.1109/TAP.2017.2712183, 2017.